ELSEVIER

Diamond and Related Materials 8 (1999) 1377–1382

DIAMOND AND RELATED MATERIALS

www.elsevier.com/locate/diamond

Molecular beam mass spectrometry studies of the gas-phase chemistry occurring during microwave plasma assisted chemical vapour deposition of diamond

S.M. Leeds *, P.W. May, E. Bartlett, M.N.R. Ashfold, K.N. Rosser

School of Chemistry, University of Bristol, Cantock's Close, Bristol BS8 1TS, UK

Accepted 30 November 1998

Abstract

A molecular beam mass spectrometer has been used for in-situ studies of the gas-phase composition during microwave plasma chemical vapour deposition of diamond, in a way that decouples the gas-phase reactions from those occurring near the substrate surface.

The system has been used to examine the plasma composition for a variety of hydrocarbon precursor-in-H_2 feedstock gas mixtures. Stable hydrocarbon species, and the methyl radical signal, were recorded and calibrated to give mole fractions of all the carbon-containing species present at detectable levels. The plasma composition has been studied with varying chemical vapour deposition process parameters such as applied microwave power, and concentration of hydrocarbon in the feed gas. Molecular beam mass spectrometry has also been used to determine the plasma gas temperature, yielding results in good agreement with non-invasive methods. © 1999 Elsevier Science S.A. All rights reserved.

Keywords: Gas-phase chemistry; Microwave plasma; Molecular beam mass spectrometry

1. Introduction

Molecular beam mass spectrometry (MBMS) is a useful technique for the analysis of gas-phase environments such as flames and plasmas. Its strength lies in the ability to detect simultaneously both stable species and highly reactive entities such as radicals. It is possible to determine absolute concentrations of stable species from the data by calibration at room temperature with a known quantity of each stable gas.

MBMS has been used to study chemistry in hot filament CVD reactors, initially by Hsu [1,2], and later at Bristol [3–5]. Hsu's sampling technique was to extract gases via an orifice in the substrate, and thus was able to analyse the composition of the flux incident at the growing diamond surface. Hsu also studied microwave plasma CVD (MWCVD) in the same reactor [6,7]. Here, we report the design and implementation of MBMS to sample gases from the side of a microwave plasma, similar to the arrangement previously used for the hot filament chemical vapour deposition (HFCVD) system in our laboratory [3–5,8]. This allows probing of the gas-phase chemistry in isolation, with minimum perturbation from gas–surface reactions.

2. Experimental

Fig. 1 shows a schematic diagram of our system. An ASTeX 1.5 kW (2.45 GHz) microwave generator is coupled to a custom-built reactor chamber containing a substrate holder mounted on a vertical translation stage. The substrate is heated electrically by a graphite element encased in the molybdenum substrate holder. Typical deposition parameters are: 0–4% CH_4 in H_2 at 20 Torr, 200 sccm total gas flow rate, 1000 W microwave power, and ~1000°C substrate temperature. Reactant gases pass through mass flow controllers (Tylan General), and the gas mixture enters the chamber via an inlet close to the quartz window. The gases flow through the reaction zone and are pumped away at the bottom of the reactor (volume $0.02\,m^3$). A substrate was not present during the experiments described here. A substrate holder temperature of ~1000°C was maintained during these experiments.

---

* Corresponding author. Fax: +44 117-9251295.
E-mail address: stuart.leeds@bristol.ac.uk (S.M. Leeds)

PII: S0925-9635(99)00014-X

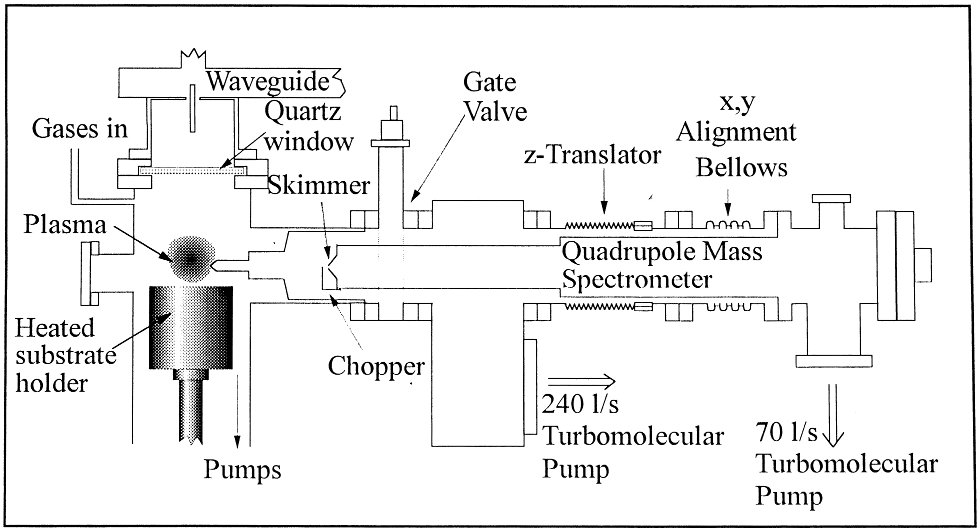

Fig. 1. Schematic diagram showing the molecular beam mass spectrometer attached to the microwave plasma CVD chamber (not to scale).

A pencil-shaped molybdenum probe, the main body of which is 10 mm in diameter (8 mm inside diameter), is used to extract gas from the side of the plasma. The probe tip is a truncated cone (outside angle 45°, top diameter <500 μm). The probe extends to 15 mm from the reactor's vertical axis and has a 100 μm extraction orifice laser drilled into its centre. Probes fabricated from quartz and stainless steel were also investigated, but these proved unsatisfactory. Quartz probes were rapidly etched by the plasma so the orifice enlarged too quickly to gather results, while stainless-steel probes developed a graphitic coating that regularly blocked the orifice. In contrast, the molybdenum probe gradually becomes coated with diamond during use, which reduces the orifice radius at a rate concomitant with typical diamond growth rates in this system (~ 0.3 μm h^{-1}). This necessitated removal of the probe for re-drilling after every 20 h or so, to maintain an approximately constant orifice diameter. During operation, the probe glows orange due to the heating effect of the plasma. The temperature of the probe is estimated to be ~ 1000°C, as its colour is similar to that of the substrate holder at this temperature. For similar probe geometry and dimensions, the shape and extent of the plasma ball appear insensitive to the electrical conductivity of the material from which the probe is fabricated. The reflected power level is unchanged by the presence of the probe. These observations encourage the belief that the probe does not pose a significant perturbation to the plasma environment.

The sampling orifice leads to the first stage of mass spectrometer differential pumping. The large pressure differential across the orifice ($>20\,000{:}1$) creates a supersonic gas expansion into the mass spectrometer first stage, rapidly 'freezing' chemical reactions in the extracted gas [2]. A 1 mm skimmer orifice ~ 100 mm downstream of the sampling orifice collimates the expansion, forming a molecular beam in the mass spectrometer second stage (base pressure $<5\times10^{-8}$ Torr, $<2\times10^{-6}$ Torr during operation), which houses the quadrupole mass spectrometer (Hiden Analytical PIC 3F). The mass spectrometer and associated vacuum technology is the same as that used in the previous studies of HFCVD [3–5,8]. The electron ionizer energies used to detect each species were: H_2 and CH_4 16.0 eV, C_2H_2 13.2 eV (to minimize signal due to cracking from C_2H_4 occurring above 13.5 eV), C_2H_4 11.9 eV (to avoid possible detection of residual N_2 above 15.5 eV, and CO above 14.0 eV), and CH_3 13.6 eV (to reduce signal due to cracking from CH_4 above 14.3 eV).

Data collected from the mass spectrometer were corrected for temperature dependence of the orifice throughput, and a background subtraction for residual gas in the mass spectrometer was performed. The data for each species were then calibrated with a known amount of each stable species to give its mole fractions. These correction and calibration procedures are identical to those applied in previous HFCVD studies [3–5,8].

3. Results and discussion

3.1. *Microwave power variation*

Plasma composition was examined as a function of applied microwave power. The results for CH_4, C_2H_2, and C_2H_4 source gases in H_2 are shown in Fig. 2a–c, respectively. An input C:H_2 ratio of 0.02 was used in all three cases. Errors in the data are typically $\sim 5\%$ for CH_4 and C_2H_2, $\sim 30\%$ for CH_3 and $\sim 50\%$ for C_2H_4. The data presented are corrected for the temperature dependence of the orifice throughput, but the

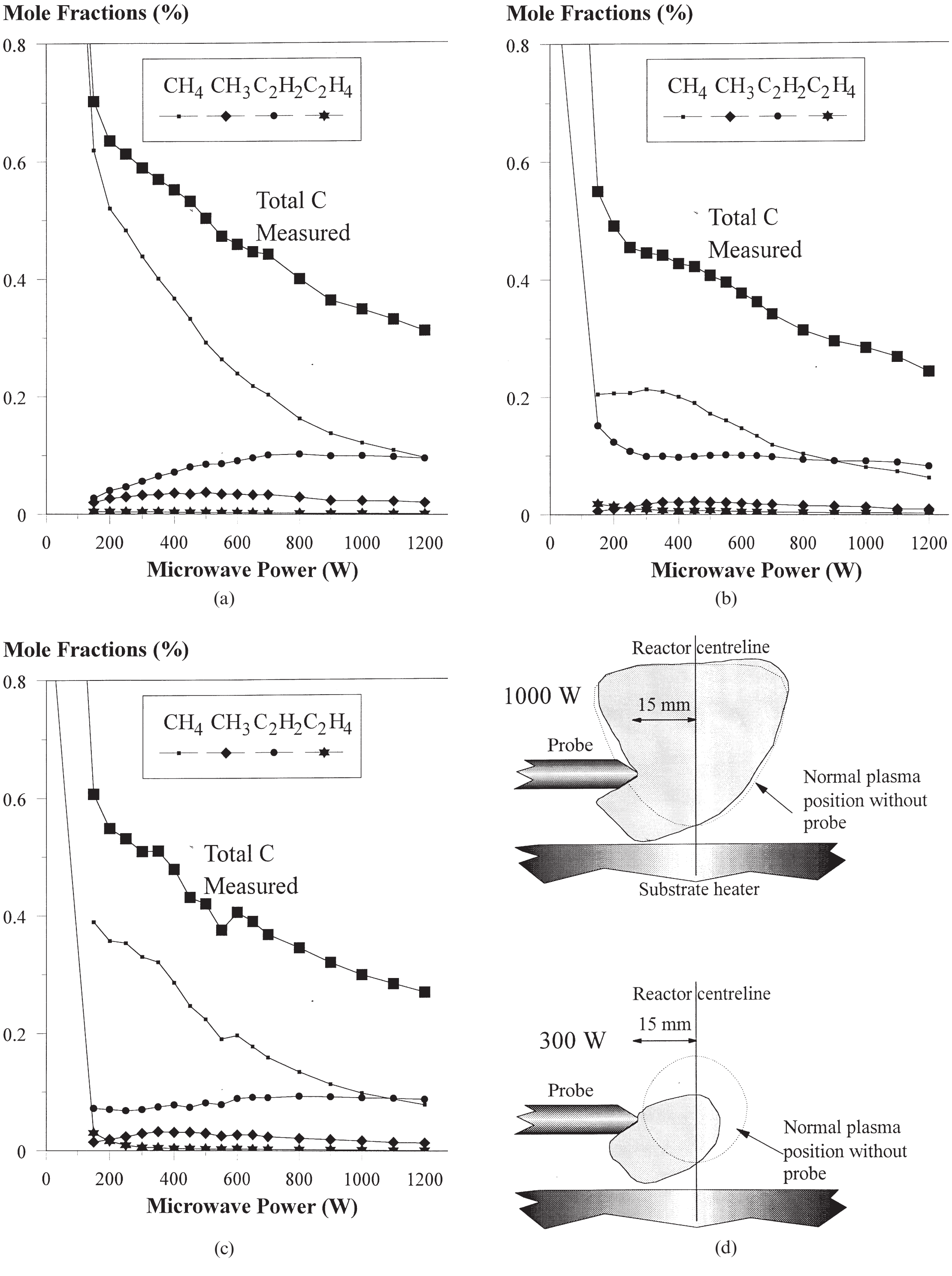

Fig. 2. Hydrocarbon species concentrations measured by in-situ MBMS as a function of applied microwave power. All results were obtained at 20 Torr, 200 sccm total gas flow rate, with a substrate temperature ~1000°C, with the probe tip ~20 mm above the substrate and 15 mm from the centre of the reactor. A C:H_2 ratio of 2% was used for (a)–(c). (a) 2% CH_4 source gas in H_2. (b) 1% C_2H_2 source gas in H_2.(c) 1% C_2H_4 source gas in H_2. (d) An approximate indication of the plasma position for two applied microwave power levels representative of the data in (a)–(c).

measured carbon total does not sum to the input 2%. This effect makes comparison with other authors' data difficult. Similar observations have been reported previously for HFCVD [2,3,9], where this effect was ascribed to thermal diffusion. Steep temperature gradients, necessary for thermal diffusion, are predicted near the plasma edge in the models of Rau et al. [10–12].

Interpretation of the data shown in Fig. 2 is further complicated by the fact that the size of the plasma ball changes with applied microwave power. Fig. 2d gives an approximate indication of the size and location of the luminous plasma ball for two representative power levels. At low powers, we sample from a point closer to the plasma edge, whereas at high powers, a point deeper in the plasma is sampled. As Fig. 2 demonstrates, the measured plasma composition is essentially independent of the source gas used at high microwave powers. At low powers, CH_4 is the most abundant hydrocarbon, even for C_2H_2 and C_2H_4 source gases. With increasing power, we see a conversion from CH_4 to C_2H_2, the mole fractions of which become comparable at the highest powers used. Very little C_2H_4 and no C_2H_6 were detected under all conditions studied. These trends mimic those seen during hot filament CVD over a filament temperature range of ~2000–2800 K [3], but the present MWCVD results suggest lower CH_3 mole fractions than during HFCVD studies [8]. More detailed comparison between the microwave plasma and hot filament systems is complicated by the difficulties in comparing local gas temperatures in the two systems. Also, definition of the sampling probe position is trivial in a HFCVD reactor, but there is no comparable solid surface in a diffuse plasma. However, we have developed a method to determine the gas temperature of the plasma gas sampled in this work.

3.2. Plasma temperature measurements

The fact that the orifice sampling efficiency (gas throughput) is temperature-dependent [1,3] suggests a route for determining the temperature, T_g, of the sampled gas. The mass spectrometer signal for argon in a 2% Ar-in-H_2 gas mixture was found to scale as $T_g^{-1.6}$ [3,8]. We have used this relationship to extract temperature information from a 2% Ar-in-H_2 plasma. For calibration, we used the room-temperature signal for 2% Ar-in-H_2, measured prior to generating the plasma. The results are presented in Fig. 3. The assumption made in the use of this relationship is that the dilute Ar-in-H_2 mixture has the same thermal properties when heated by a plasma as when heated by a hot filament. The temperatures measured by this technique compare well with the results of Lang et al. [13], who used H_2 visible emission spectroscopy to determine the neutral gas temperature of a 1% CH_4-in-H_2 plasma. They reason that the Doppler temperature of H_2 can give a reliable measure of the neutral gas temperature. Their gas temperatures determined by this method for a range of microwave powers were measured at a pressure of 80 mbar. Fig. 2 of Ref. [13] shows a linear correlation between gas temperature and reactor pressure. Extrapolation to our working pressure of 20 Torr (~27 mbar) suggests a reduction in T_g of 600 K. Adopting this correction, their data have also been included in Fig. 3 and are in excellent accord with the present results. So too is the work of Weimer et al. [14], who measured a maximum gas temperature of 1100 K for a 170 W microwave plasma using a shielded thermocouple. The agreement between the non-intrusive (optical) techniques and the present results reinforces our assumption that the presence of the sampling probe does not appreciably affect the sampled gas.

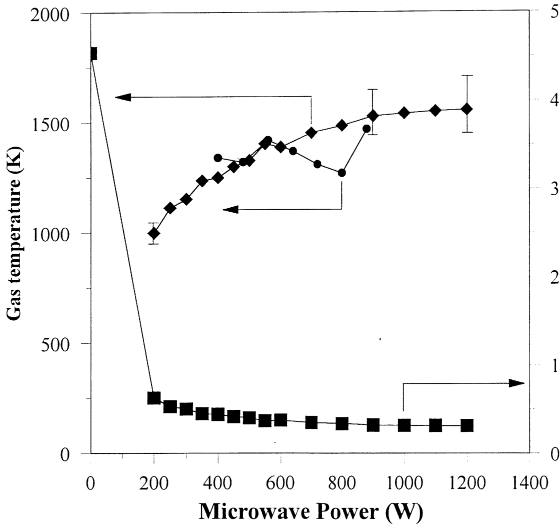

Fig. 3. Plasma-gas temperature determined in a 2% Ar-in-H_2 plasma under identical CVD process conditions to the data in Fig. 2. ■: the Ar signal (counts per second, c s^{-1}) measured by the mass spectrometer. ◆: gas temperature calculated from the Ar signal. ●: results of Lang et al. [13], which have been extrapolated to our process conditions (see Section 3.2 for discussion).

We have also used a second probe 10 mm shorter than that used for all other experiments in this paper, which samples outside the visible plasma edge for microwave power levels <600 W. Sampled gas temperatures measured using the Ar-in-H_2 method described above are substantially lower (~400 K) at low microwave powers, but rise rapidly at the highest powers as the visible plasma ball extends to encompass the probe tip, indicating a drop of ~1000 K over 10 mm in the vicinity of the plasma edge. This is evidence for a significant temperature gradient that may be responsible for the observed mass-dependent thermal diffusion effects (Sections 3.1 and 3.3).

3.3. Variation of hydrocarbon concentration

The concentration of each hydrocarbon source gas has been varied, and Fig. 4 shows an example where CH_4-in-H_2 is used at a constant power of 1000 W at 20 Torr. The equivalent graphs for C_2H_4 and C_2H_2 overlay these curves, and are not shown. This agrees with Fig. 2, which shows that at high powers, the plasma composition is independent of the carbon source gas identity. When repeated using lower powers, the depen-

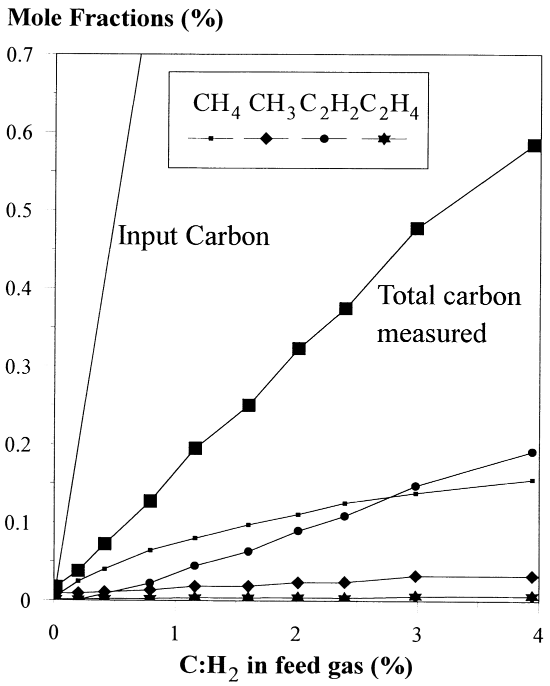

Fig. 4. Effect of C:H ratio of input gases on plasma composition. All results were obtained at 20 Torr, 200 sccm total gas flow rate, with a substrate temperature ~1000°C, with the probe tip ~20 mm above the substrate and 15 mm from the centre of the reactor. Note also that the measured carbon total is always less than the input carbon mole fraction, as discussed in Sections 3.1 and 3.3.

dence of the plasma composition on source gas manifests itself as a splitting of the curves for each source gas, in the manner of Fig. 2a–c. The methyl radical is the most abundant hydrocarbon in the plasma (after CH_4) for methane concentrations $<0.4\%$, corresponding to the region where the highest quality CVD diamond is grown [15,16]. $[C_2H_2]$ increases dramatically as the amount of carbon in the feed is increased. As expected, we do not see the filament surface saturation effects noted during hot filament CVD [2] where the carbon source becomes the most prevalent hydrocarbon at high input carbon concentrations. The data in Fig. 4 also reveal that $[C_2H_2] \propto [CH_3]^2$, indicating that atomic hydrogen must be present in the plasma at a sufficiently high concentration to convert C_2H_6 rapidly to C_2H_2, as we detect no C_2H_6 and only a small quantity of C_2H_4. All of these trends mimic those reported by McMaster and Hsu (MBMS) [7], and Mitomo et al. [17] using Fourier transform infra-red spectroscopy (FTIR). However, as in Section 3.1, our measured carbon total falls considerably short of the input amount. We believe this to be due to thermal diffusion effects causing the heavier (hydrocarbon) species to diffuse away selectively from the hot plasma. Consequently they 'pile-up' in the cooler region of the gas surrounding the plasma ball. This is also the region where the substrate is generally located during CVD. The main difference between our work and that of McMaster and Hsu [7] is that they detected more acetylene and less methane at the substrate, whereas we see the converse in our plasma. At a power level of 850 W, CH_3 accounts for ~2% of the input carbon in McMaster's study [7], whereas CH_3 forms ~7% of the carbon total we measure in this work. Thus, CH_3 appears to be more abundant in the plasma than at the substrate surface. We can understand these differences since the species generated in the plasma will undergo further reactions during transport to the substrate. These reactions will involve the removal of short-lived species such as CH_3 and H, resulting in the formation of the stable species C_2H_2 (via CH_3 recombination and successive H abstractions to produce C_2H_2). The FTIR gas-phase measurements of Mitomo et al. [17] were taken on a line of sight through the plasma, and the measured carbon total was found to be consistent with the input carbon. This is to be expected since species exiting the plasma by thermal diffusion must enhance the total carbon in the cool region outside the plasma, thereby conserving the carbon total along the line of sight.

4. Conclusions

We have used MBMS in a novel sampling configuration to study gas-phase chemistry during microwave plasma CVD under a variety of experimental conditions. We find that the plasma composition becomes independent of the hydrocarbon precursor at high powers (≥700 W). At lower powers, the composition depends on the carbon source gas. The total amount of gas-phase carbon-containing species detected when the plasma was on was always significantly lower than that input. This is ascribed to thermal diffusion causing a large proportion of the hydrocarbon species to be driven from the plasma region.

MBMS has been used to determine the plasma-gas temperature, and our results show a good agreement with literature results obtained by non-invasive methods. We have related our results to those seen by MBMS at the substrate surface, and to gas-phase measurements by other techniques. These comparisons indicate relatively more CH_3 and CH_4, and less C_2H_2 in the plasma than that seen at the substrate by previous authors. We explain these differences in terms of the gas undergoing further reactions (forming C_2H_2) during transport to the substrate.

Acknowledgements

We would like to thank the EPSRC for project funding. P.W.M. would like to thank the Royal Society for the award of a University Research Fellowship.

References

[1] W.L. Hsu, D.M. Tung, Rev. Sci. Instrum. 63 (1992) 4138.
[2] W.L. Hsu, M.C. McMaster, M.E. Coltrin, D.S. Dandy, Jpn. J. Appl. Phys. 33 (4B, Part 1) (1994) 2231.
[3] C.A. Rego, P.W. May, C.R. Henderson, M.N.R. Ashfold, K.N. Rosser, N.M. Everitt, Diamond Relat. Mater. 4 (1995) 770.
[4] C.A. Rego, R.S. Tsang, P.W. May, M.N.R. Ashfold, K.N. Rosser, J. Appl. Phys. 79 (1996) 7264.
[5] R.S. Tsang, C.A. Rego, P.W. May, M.N.R. Ashfold, K.N. Rosser, Diamond Relat. Mater. 6 (1997) 247.
[6] W.L. Hsu, J. Appl. Phys. 72 (1992) 3102.
[7] M.C. McMaster, W.L. Hsu, M.E. Coltrin, D.S. Dandy, C. Fox, Diamond Relat. Mater. 4 (1995) 1000.
[8] R.S. Tsang, Ph.D. thesis, University of Bristol, 1997.
[9] E.J. Corat, D.G. Goodwin, J. Appl. Phys. 74 (1993) 2021.
[10] H. Rau, F. Picht, J. Mater. Res. 8 (1993) 2250.
[11] H. Rau, B. Trafford, J. Phys. D 23 (1990) 1637.
[12] H. Rau, F. Picht, J. Phys. D 26 (1993) 1260.
[13] T. Lang, J. Stiegler, Y. von Kaenel, E. Blank, Diamond Relat. Mater. 5 (1996) 1171.
[14] W.A. Weimer, F.M. Cerio, C.E. Johnson, J. Mater. Res. 6 (1991) 2134.
[15] S.M. Leeds, T.J. Davis, P.W. May, C.D.O. Pickard, M.N.R. Ashfold, Diamond Relat. Mater. 7 (1998) 233.
[16] S.M. Leeds, Ph.D. thesis, University of Bristol, 1999.
[17] T. Mitomo, T. Ohta, E. Kondoh, K. Ohtsuka, J. Appl. Phys. 70 (1991) 4532.